Novel Foot Progression Angle Algorithm Estimation via Foot-Worn, Magneto-Inertial Sensing

Yangjian Huang, Wisit Jirattigalachote, *Student Member, IEEE,* Mark R. Cutkosky, Xiangyang Zhu, and Peter B. Shull*, *Member, IEEE*

***Abstract*—*Objective*: The foot progression angle is an important clinical measurement but currently can only be computed while walking in a laboratory with a marker-based motion capture system. This paper proposes a novel foot progression angle estimation algorithm based on a single integrated sensor unit, consisting of an accelerometer, gyroscope, and magnetometer, worn on the foot. *Methods*: The algorithm introduces a real-time heading vector with a complementary filter and utilizes a gradient descent method and zero-velocity update correction. Validation testing was performed by comparing foot progression angle estimation from the wearable sensor with the standard foot progression angles computed from a marker-based motion capture system. Subjects performed nine walking trials of 2.5 minutes each on a treadmill. During each trial, subjects walked at one speed out of three options (1.0 m/s, 1.2 m/s, and 1.4 m/s) and walked with one gait pattern out of three options (normal, toe-in, and toe-out). *Results*: The algorithm estimated foot progression angle to within 0.2° of error or less for each walking conditions. *Conclusion*: A novel foot progression angle algorithm has been introduced and described based on a single foot-worn sensor unit, and validation testing showed that foot progression angle estimation was accurate for different walking speeds and foot angles. *Significance*: This work enables future wearable systems gait research to assess or train walking patterns outside a laboratory setting in natural walking environments.**

***Index Terms*—Complementary filter, position and orientation tracking, zero velocity update.**

I. Introduction

THE foot progression angle is an important gait-related, clinical measurement. Abnormal foot progression angle is a clinical indicator of cerebral palsy [1], and gait re-training which alters foot progression angle has been shown to reduce knee loading and knee pain for individuals with knee osteoarthritis [2], [3]. Other clinical applications include monitoring gait in patients with distal tibial physeal fractures [4] or clubfoot [5]. In addition, changes in the foot progression angle have been correlated with changes in foot eversion moment [6], knee adduction moment [7], [8], hip joint moment [9], foot pressure distribution [10], and foot medial loading [11].

Y. Huang and X. Zhu are with the State Key Laboratory of Mechanical System and Vibration, School of Mechanical Engineering, Shanghai Jiao Tong University, Shanghai, 200240 China.

W. Jirattigalachote and M. R. Cutkosky are with the Department of Mechanical Engineering, Stanford University, Stanford, CA, 94305 USA.

*P. B. Shull is with the State Key Laboratory of Mechanical System and Vibration, School of Mechanical Engineering, Shanghai Jiao Tong University, Shanghai, 200240 China (e-mail: pshull@sjtu.edu.cn).

Foot-worn sensing has been used to estimate a variety of gait parameters. Pappas et al. [12] introduced a gait phase detection system to detect stance, heel-off, swing, and heel-strike with a gyroscope and three force sensitive resistors. Sabatini et al. [13] developed an inertial measurement system (IMU) for estimating spatio-temporal gait parameters including stride time, stride length, walking speed, incline and relative stance. Rebula et al. [14] used IMUs to estimate stride length, width, period, and variability. Rouhani et al. [15] used a foot-worn IMU to estimate relative foot and ankle kinematics including dorsi-flexion/plantar-flexion, inversion/eversion, and internal/external rotation. Mariani et al. [16] assessed gait and turning for patients with parkinson's desease via shoe-worn sensors. Tien et al. [17] used IMUs to detect foot kinematics to facilitate diagnosing neurological disorders. Finally, Schepers et al. [18] and Rouhani et al. [19] assessed ankle and foot kinetics including 3D force, moment and power of joint with inertial sensors and force transducers. Previous research has shown that wearable sensors can be used to track walking trajectories over time. Meng et al. [20] used inertial and magnetic sensors worn on the foot to estimate pedestrian walking trajectories by introducing a velocity control variable to bound velocity drift and stride-based position pseudomeasurements to feed an adaptive Kalman filter for position estimation. Yun et al. [21] used an adaptive-gain complementary filter to estimate position by integrating acceleration data whose drift was corrected through zero velocity updates, and Kwanmuang et al. [22] combined IMU and magnetometer measurements and used heuristic methods to estimate walking trajectories.

Several algorithms have been proposed to estimate gait parameters with foot-worn sensing. Sabatini et al. [23] proposed a quaternion-based extended Kalman filter to estimate orientation. Madgwick et al. [24] introduced the gradient descent algorithm to compensate for gyroscope integration error by using accelerometer and magnetometer signals and quaternion derivatives. Skog et al. [25] derived a general foot stance phase detector for zero-velocity update to address drift problems for foot-mounted inertial navigation. Finally, Mariani et al. [26] computed heel-strike and toe-off gait events from kinematic features estimated from foot-worn inertial sensors.

While wearable sensors and algorithms have enabled the estimation of a variety gait characteristics [27], a critical missing parameter is the foot progression angle. One challenge is that the foot progression angle is not a measurement relative to other body segment kinematics but rather relative to the subject's walking direction. To solve this problem, we explore using real-time estimation of a heading vector based

on trajectory estimation as a kinematic reference.

The purpose of this paper is to present a novel algorithm for estimating the foot progression angle by using a single magneto-IMU (3-axis accelerometer, 3-axis gyroscope, 3-axis magnetometer) worn on the foot and combining computed heading vectors and foot vectors. We anticipated such an approach would not be prone to drift and would be accurate to within a few degrees. For validation, we compared sensor estimation results with measurements from an optical motion capture system.

II. Foot Progression Angle Estimation

The foot progression angle is defined by the angle between the foot vector and the heading vector (line of walking progression) [28]. The foot progression angle algorithm is composed of six components (Fig. 1). Orientation is estimated via the gradient descent algorithm [24], trajectory is estimated via strapdown integration [29], and stance phase identification is used with zero-velocity detection [25] to correct velocity estimation drifts. The heading vector and foot vector are computed based on results of trajectory and orientation estimation, respectively, and the foot progression angle is the difference between these vectors in the horizontal plane.

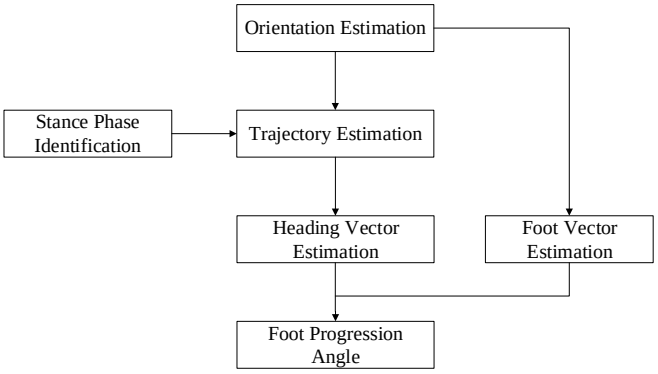

Fig. 1. Foot progression angle algorithm flowchart.

A. Orientation and Trajectory Estimation

We estimate sensor orientation with respect to the earth frame ${}^{S}_{E}q$ by integrating angular velocity from the gyroscope and then applying gradient descent correction with accelerometer and magnetometer data to get drift-reduced orientation estimation (Fig. 2A).

The process begins by calculating the quaternion derivative:

$$ {}^{S}_{E}\dot{q}_{\omega,t} = \frac{1}{2} {}^{S}_{E}q_{est,t-1} \otimes {}^{S}\omega_t * \Delta t \tag{1} $$

where ${}^{S}_{E}q_{est,t-1}$ is the previous time step orientation estimation, ${}^{S}\omega_t = [0\ \omega_x\ \omega_y\ \omega_z]$ comes from the gyroscope, Δt is the sampling period, and $\otimes$ is the quaternion multiplication operator [30]. We use the following notation throughout this paper: the left superscript is the frame in which the vector is described, for example, ${}^{S}\omega_t$ describes the gyro's reading in sensor frame. A leading superscript denotes the frame being described in and a leading subscript denotes the frame this is with reference to, for example, ${}^{S}_{E}\dot{q}_{\omega,t}$ describes the orientation change rate of sensor frame relative to earth frame. The right subscript i indicates stride number, and the right subscript t indicates time step.

To improve orientation estimation with the information from the accelerometer and magnetometer, we implement a gradient descent method similar to that presented in Madgwick [24]. Gravity sensed via the accelerometer provides correction for gyroscope drift caused by the tilt angle and magnetic north sensed via the magnetometer provides correction for gyroscope drift about the superior-inferior axis.

Then equation 2 adjusts the rate of change of orientation estimate from the gyroscope (${}^{S}_{E}\dot{q}_{\omega,t}$) by removing the magnitude of the gyroscope measurement error (β) in the gradient direction based on accelerometer and magnetometer information [24].

$$ {}^{S}_{E}\dot{q}_{est,t} = {}^{S}_{E}\dot{q}_{\omega,t} - \beta \frac{\nabla \mathbf{f}}{||\nabla \mathbf{f}||} \tag{2} $$

The gyroscope measurement error is an adjustable parameter defined as:

$$ \beta = \| \frac{1}{2} \hat{q} \otimes [0 \quad \tilde{\omega}_{max} \quad \tilde{\omega}_{max} \quad \tilde{\omega}_{max}] \| = \sqrt{\frac{3}{4}} \tilde{\omega}_{max} \tag{3} $$

where $\tilde{\omega}_{max}$ represents the maximum gyroscope measurement error of each axis and $\hat{q}$ is any unit quaternion.

The esimated orientation ${}^{S}_{E}q_{est,t}$ is calculated by numerically integrating the estimated rate of change of orientation:

$$ {}^{S}_{E}q_{est,t} = {}^{S}_{E}q_{est,t-1} + {}^{S}_{E}\dot{q}_{est,t} * \Delta t \tag{4} $$

From equation 2, the expression $\mathbf{f}$ represents the orientation correction from accelerometer and magnetometer data. The generic formulation for finding orientation from the sensor to earth frame (${}^{S}_{E}\hat{q} = [q_1\ q_2\ q_3\ q_4]$), is to predefine a reference direction of the earth frame (${}^{E}\hat{d} = [0\ d_x\ d_y\ d_z]$) and measure sensor data in the sensor frame (${}^{S}\hat{s} = [0\ s_x\ s_y\ s_z]$). Then solve equation 5 using the objective function $\mathbf{f}$ from equation 6.

$$ \min_{{}^{S}_{E}\hat{q} \in \mathbb{R}^4} \mathbf{f}({}^{S}_{E}\hat{q}, {}^{E}\hat{d}, {}^{S}\hat{s}) \tag{5} $$

$$ \mathbf{f}({}^{S}_{E}\hat{q}, {}^{E}\hat{d}, {}^{S}\hat{s}) = {}^{S}_{E}\hat{q}^* \otimes {}^{E}\hat{d} \otimes {}^{S}_{E}\hat{q} - {}^{S}\hat{s} \tag{6} $$

By applying a gradient descent method, we define:

$$ \nabla \mathbf{f}({}^{S}_{E}\hat{q}_k, {}^{E}\hat{d}, {}^{S}\hat{s}) = \mathbf{J}^T({}^{S}_{E}\hat{q}_k, {}^{E}\hat{d}) \mathbf{f}({}^{S}_{E}\hat{q}_k, {}^{E}\hat{d}, {}^{S}\hat{s}) \tag{7} $$

where $\mathbf{J}$ is the Jacobian of function $\mathbf{f}$.

Then, for the accelerometer estimation case, we substitute ${}^{E}\hat{g} = [0\ 0\ 0\ 1]$ for ${}^{E}\hat{d}$ and ${}^{S}\hat{a} = [0\ a_x\ a_y\ a_z]$ for ${}^{S}\hat{s}$, where ${}^{E}\hat{g}$ is the gravity vector and ${}^{S}\hat{a}$ is the accelerometer data in the sensor frame. Similarly, for the magnetometer, we substitute ${}^{E}\hat{b} = [0\ b_x\ 0\ b_z]$ for ${}^{E}\hat{d}$ and ${}^{S}\hat{m} = [0\ m_x\ m_y\ m_z]$ for ${}^{S}\hat{s}$, where ${}^{E}\hat{b}$ represents a normalized magnetic vector and ${}^{S}\hat{m}$ is the magnetometer data in the sensor frame.

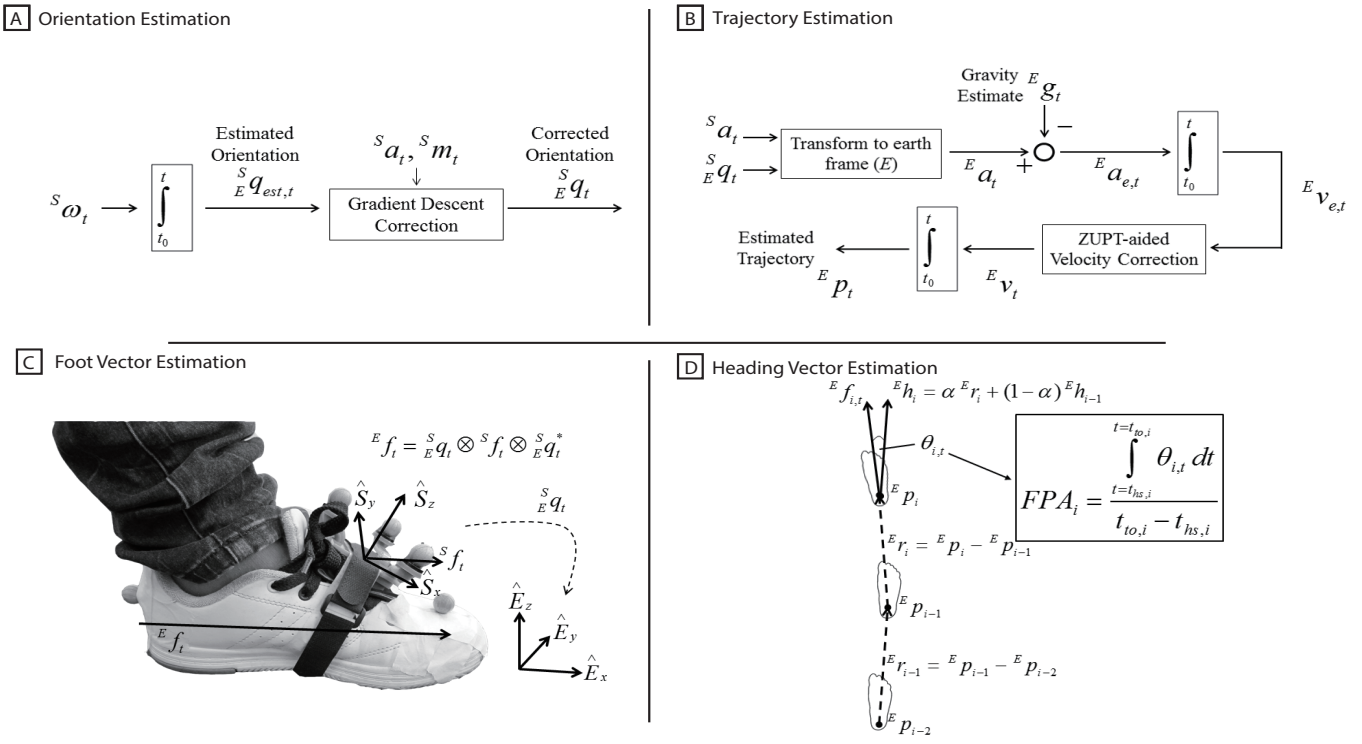

Fig. 2. Foot progression angle estimation procedure: (A) Sensor orientation with respect to the earth frame E is calculated by integrating angular velocity and corrected with information from the accelerometer and magnetometer. (B) The foot trajectory is computed through double integration of the acceleration in the earth frame and is corrected via the zero-velocity assumption during stance. (C) The foot vector is fixed with respect to the sensor frame S, then is transformed into the earth frame using the corrected orientation estimated from the previous step. (D) The heading vector is computed via a complementary filter applied to the foot trajectory at each stride. Finally, the foot progression angle (FPA) is computed as the difference between the heading vector and foot vector integrated over the stance phase of each step.

The objective function of the combined systems becomes equation 8 and the combined Jacobian is equation 9. Subscript g indicates that the given function is based on accelerometer data while subscript b indicates magnetometer data.

$$\mathbf{f}_{g,b}({}^S_E\hat{q}, {}^S\hat{a}, {}^E\hat{b}, {}^S\hat{m}) = \begin{bmatrix} \mathbf{f}_g({}^S_E\hat{q}, {}^S\hat{a}) \\ \mathbf{f}_b({}^S_E\hat{q}, {}^E\hat{b}, {}^S\hat{m}) \end{bmatrix} \tag{8}$$

$$\mathbf{J}^T_{g,b}({}^S_E\hat{q}, {}^E\hat{b}) = \begin{bmatrix} \mathbf{J}^T_g({}^S_E\hat{q}) \\ \mathbf{J}^T_b({}^S_E\hat{q}, {}^E\hat{b}) \end{bmatrix} \tag{9}$$

Thus, we find

$$\nabla\mathbf{f} = \begin{cases} \mathbf{J}^T_g({}^S_E\hat{q})\ \mathbf{f}_g({}^S_E\hat{q}, {}^S\hat{a}) \\ \mathbf{J}^T_{g,b}({}^S_E\hat{q}, {}^E\hat{b})\ \mathbf{f}_{g,b}({}^S_E\hat{q}, {}^S\hat{a}, {}^E\hat{b}, {}^S\hat{m}) \end{cases} \tag{10}$$

Now, by applying equations 4, 2, 1, 3 and 10, we determine the corrected orientation ${}^S_E q_{est,t}$ (Fig. 2A).

Once the corrected sensor orientation is computed, we use this orientation to transform the acceleration data into a body acceleration in the earth frame. Then, we double integrate it to estimate the trajectory of the foot (${}^E p_i$). During this process, a zero-velocity update correction (ZUPT) [25] based on stance phase identification is deployed to reduce drift from velocity integration (Fig. 2B).

B. Stance Phase Identification

During the stance phase of gait the foot is relatively stationary with respect to the ground, assuming no foot slip occurs. We use zero-velocity estimation [25] based on acceleration and gyroscope information to help estimate the stance period and implement a state-machine based approach similar to Yun, et al. [21] for improved identification accuracy. In addition, we use the heel strike events detected and approximate the stance phase duration as 60% of the stride time.

C. Foot Vector Estimation

The foot vector (${}^S f$) is estimated as the common vector fixed in an IMU-sensor frame (S) (Fig. 2C), similar to the method performed by Favre, et al. [31]. Each subject performs dorsiflexion and plantarflexion motion of the ankle slowly three times, in order to find a common rotation axis (${}^S k$). The gravity axis (${}^S g$) can be approximated from the accelerometer data when the foot is flat on the ground. Using the right hand rule, we compute the foot vector as

$${}^S f = {}^S k \times {}^S g \tag{11}$$

Then, the sensor orientation ${}^S_E q_t$ previously found is applied to form the foot vector in an estimated earth frame (${}^E f_t$).

$${}^E f_t = {}^S_E q_t \otimes {}^S f_t \otimes {}^S_E q_t^* \tag{12}$$

D. Heading Vector Estimation

The heading vector estimates the direction of forward movement (Fig. 2D). At each i^{th} heel strike, a foot trajectory ($^{E}p_i$) is calculated. Then, a temporary heading vector ($^{E}r_i$) is estimated by subtracting the foot trajectory from the previous heel strike.

$$^{E}r_i = {}^{E}p_i - {}^{E}p_{i-1} \tag{13}$$

Then, the heading vector is computed as:

$$^{E}h_i = \alpha {}^{E}r_i + (1-\alpha){}^{E}h_{i-1} \tag{14}$$

where $^{E}h_i$ is the heading vector at the i^{th} stride and α is a complementary filter parameter.

E. Foot Progression Angle

The foot progression angle is computed as the average angle between the foot vector and heading vector during stance (Fig. 2D). The foot vector is computed at each time step t, while the heading vector is estimated at each stride i after heel strike. At each time step t, an angle is defined between the foot vector and the heading vector projected onto horizontal plane parallel with the ground:

$$\theta_{i,t} = \angle({}^{E}f_{i,t}, {}^{E}h_i) \tag{15}$$

And the foot progression angle for each step is the average of this angle during stance:

$$FPA_i = \frac{\int_{t_{hs,i}}^{t_{to,i}} \theta_{i,t} dt}{t_{to,i} - t_{hs,i}} \tag{16}$$

where FPA_i is a foot progression angle evaluated for each step, $\theta_{i,t}$ is a foot progression angle for time step t, $t_{hs,i}$ is the start of the stance period, $t_{to,i}$ is the end of the stance period, and the subscript i represents the i^{th} stride. In addition, to avoid transient foot progression angle estimates near heel strike and toe-off events, values were averaged from 20% to 80% of stance during which FPA is relatively constant [32].

III. Experimental Validation

To quantify the accuracy of the algorithm, we performed subject testing with a wearable sensor to compute the foot progression angle and compared this with the foot progression angle measurement from an optical motion capture system. Thirteen subjects (10 male/3 female, 30.4±12.0 years, 1.74±0.07 m, 66.2±10.0 kg) participated in this study which was performed in accordance with the Declaration of Helsinki. Each subject wore a custom-designed module consisting of a microcontroller (atmega328, Atmel, CA, USA), 3-axis accelerometer and 3-axis gyroscope (MPU6050, Invensense, CA, USA), 3-axis magnetometer (HMC5883L, Honeywell, MN, USA), and a 400 mAh Li-Po rechargeable battery. The dimensions of this integrated wearable sensing module are 37.0 mm×31.0 mm×17.5 mm (Fig. 3). A 3 cm wide velcro strap was used to attach the sensor system to the top of the foot and was wrapped around the narrowest part of the foot to minimize the relative motion between the sensor and the subject's foot. A piece of 5 mm-thick soft neoprene was placed between the sensor and foot to minimize high frequency errors from sensor jolting [13].

Fig. 3. Wearable magneto-inertial sensing system (37.0 mm×31.0 mm×17.5 mm) is put in a small plastic case and strapped to the shoe for testing. Optical motion capture markers are attached to sensor module case for validation testing.

Raw sensor data from the wearable system were sampled at 100 Hz and streamed to a computer via a Bluetooth module (RN41, Roving Networks, AZ, USA). Motion capture data were also collected at 100 Hz via an eight-camera motion capture system (Vicon, Oxford Metrics Group, Oxford, UK) as subjects walked on a treadmill (Bertec, Ohio, USA). Each system time-stamped data locally based on their respective on-board timers. Because it was not feasible to start data collection on both systems at exactly the same instant, a short pulse was recorded on the wearable system and simultaneously sent from the wearable system to the motion capture system via a cable (negligible transmission delay) at the start of each trial prior to walking so that data collected from the two systems could be synced and analyzed during post-processing.

At the beginning of the experiment, subjects performed a static calibration trial, standing still with both feet together, pointing forward for 10 seconds to find the gravity axis. Then subjects lifted their foot and slowly dorsiflexed and plantarflexed three times to find the estimated common rotation axis. Also, during the static trial the earth frame relative to the sensor frame is determined such that $-\hat{E}_z$ is defined by the gravity vector, $\hat{E}_x$ is defined to be perpendicular to the gravity vector in the direction of the magnetic north pole, and $\hat{E}_y$ is perpendicular to $\hat{E}_z$ and $\hat{E}_x$ according to the right-hand rule (Fig. 4). After calibration, subjects performed nine walking trials of 2.5 minutes each on the treadmill. Each trial was

a combination of three different walking speeds (1.0 m/s, 1.2 m/s, and 1.4 m/s) and three different foot progression angle gait patterns (normal, toe-in, and toe-out). Each subject performed nine total walking trials. Subjects self-selected the amount of change in foot progression angle for toe-in and toe-out gaits [33], [34].

Fig. 4. Experimental setup. Subjects performed walking trials on a treadmill while wearing a foot-mounted magneto-inertial sensor and motion capture reflective markers. S denotes the sensor reference frame and E denotes the earth reference frame.

Reflective markers were placed on the calcaneous and the head of the second metatarsal. The foot progression angle was computed in the laboratory horizontal plane as the angle between the line connecting the calcaneous and head of the second metatarsal and the line of forward progress as has been done previously [8]. Foot progression angles in which the second metatarsal head was lateral of the calcaneous were considered positive. Marker data from the motion capture system were low-pass filtered at 15 Hz using a second-order Butterworth filter. The accuracy of the presented foot progression angle algorithm was evaluated based on the average errors and RMS errors with respect to the foot progression angle computed from the motion capture system. RMS error is computed for each trial during time points of the stance phase between the magneto-IMU algorithm output and the motion capture output, and the average RMS errors are the averaged RMS errors for all trials at each given condition. Throughout the analysis, an α value of 0.35 was used in the heading vector estimation, determined based on pilot testing.

One way ANOVA was used to determine if there was any difference in errors of foot progression angle estimation based on foot orientation and one way ANOVA was also performed to determine differences based on walking speed. In the case when there was a difference, Tukey's procedure was used for post-hoc analysis. Paired Student's t-tests were used for comparing foot progression angles for each individual walking condition and bonferroni correction was used to account for multiple comparisons. Statistical significance was set to p=0.05.

IV. Results

In general, average foot progression angle estimations from magneto-IMU closely followed motion capture estimations under all walking conditions (Fig. 5). Foot progression angle estimation of stance phase from Magneto-IMU and the motion capture system during a representative trial are shown in Fig. 6. There were significant differences between magneto-IMU and motion capture foot progression angle estimates for the following walking conditions: 1.0 m/s with toe-out gait, 1.2 m/s with toe-in gait, 1.4 m/s with normal gait, and 1.4 m/s with toe-out gait, which resulted in average errors of 0.19°, 0.07°, 0.17°, 0.19° respectively.

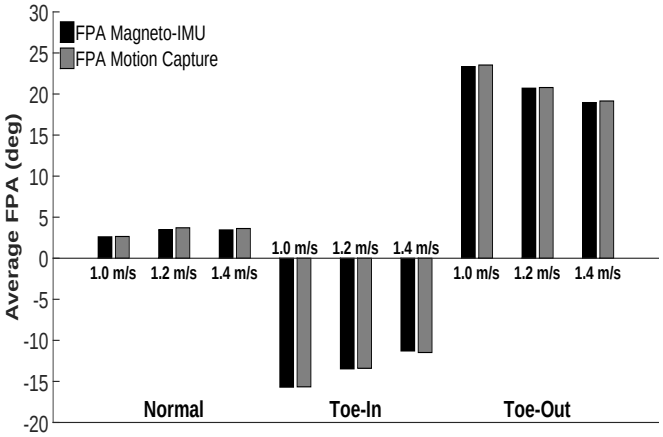

Fig. 5. Average foot progression angle (FPA) estimation from Magneto-IMU and motion capture sensing for all walking conditions. In general, average FPA estimates from Magneto-IMU sensing closely matched motion capture average FPA estimates.

Average foot progression angle errors for normal gait, toe-in gait, and toe-out gait were -0.15±0.24°, 0.03±0.41°, and -0.15±0.19°, respectively (Fig. 7) and average errors for walking speeds of 1.0 m/s, 1.2 m/s, and 1.4 m/s were -0.09±0.14°, -0.13±0.25°, and -0.05±0.44°, respectively (Fig. 8). There were no significant differences in foot progression angle estimation accuracy based on foot orientation (p=0.10) or walking speed (p=0.75). Average RMS errors for normal gait, toe-in gait, and toe-out gait were 1.84±1.45°, 2.13±1.70°, and 2.50±1.45° and average RMS errors for walking speeds of 1.0 m/s, 1.2 m/s, and 1.4 m/s were 1.92±1.35°, 2.05±1.51°, and 2.50±1.73°, respectively.[1]

[1]Specific data of average errors and RMS errors (across all subjects) for different foot orientations and walking speeds can be found in a table included as a supplementary file.

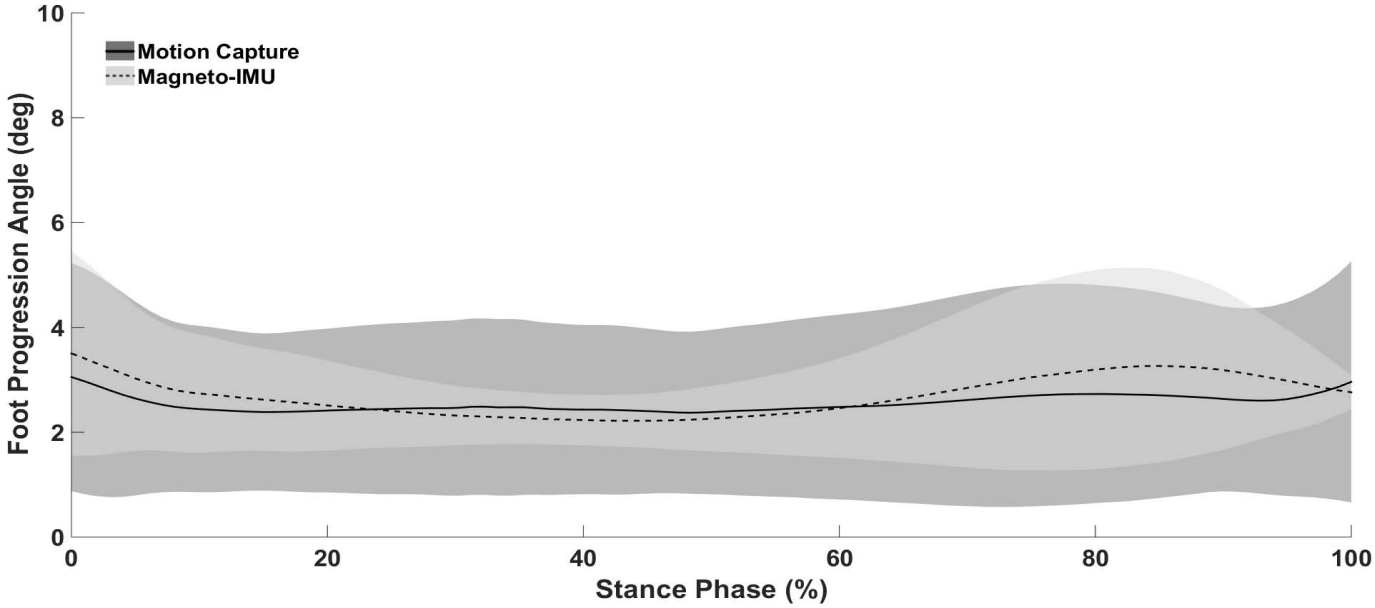

Fig. 6. Representative trial showing foot progression angle estimation from the Magneto-IMU wearable system and the reference motion capture system. The trial is for toe out gait while walking at 1.4 m/s. Solid and dashed lines represent foot progression angle estimations over stance averaged for all steps in the trial from Magneto-IMU and reference motion capture, respectively. Shading represents standard deviations of the foot progression angle from Magneto-IMU and motion capture sensing.

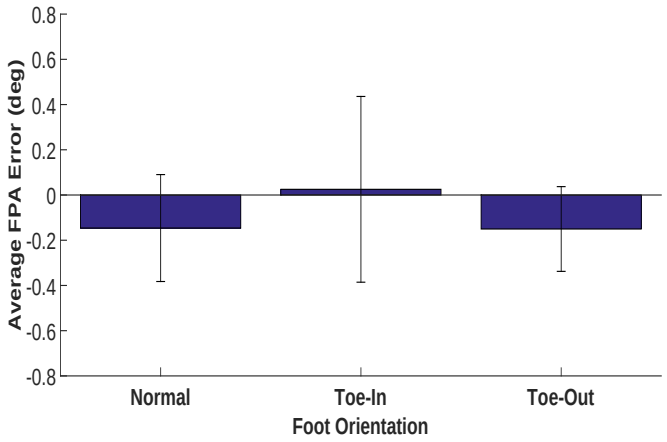

Fig. 7. Average foot progression angle (FPA) errors based on foot orientation. There were no significant differences based on foot orientation.

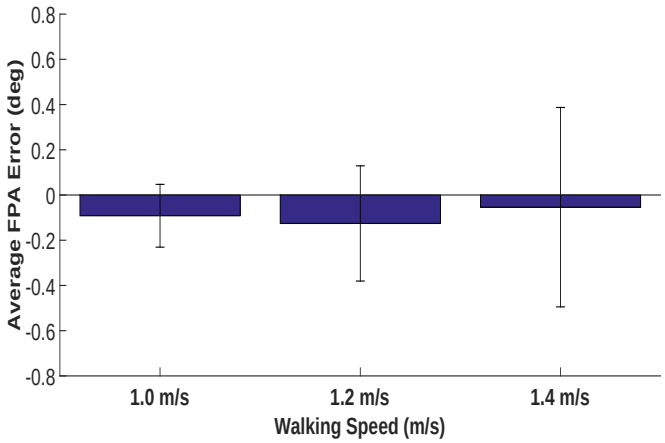

Fig. 8. Average foot progression angle (FPA) errors based on walking speed. There were no significant differences based on walking speed.

V. Discussion

The aim of this study was to develop a novel foot progression angle algorithm based on foot-worn magnetometer and inertial sensing. The proposed algorithm utilizes the gradient descent method, zero-velocity update correction and real-time foot vector and heading vector estimation. Experimental testing demonstrated the algorithm accurately estimated foot progression angle as compared to a standard motion capture system for a variety of walking conditions.

Our findings align with previous research efforts using wearable sensors for estimating gait-related kinematics. Yun et al. [21] used Magneto-Inertial system and zero velocity updates technology to estimate position and reported accuracy of 1%. Roetenberg et al. [35] presented a magnetic system (three orthogonal coils and the source) combined with inertial sensors for human motion tracking and reported accuracies of 5 mm for position and 3° for orientation. Meng et al. [20] used a Magneto-Inertial system to do trajectory tracking by introducing a velocity control variable and stride-based position pseudomeasurements as well as zero velocity updates with the average position error of 0.44 ± 0.20 m during straight line walking of 15 m and 4.31 ± 1.77 m during straight line walking of 132 m. Rouhani et al. [15] used a foot-worn IMU to estimate relative foot and ankle kinematics including dorsiflexion/plantarflexion, inversion/eversion, and internal/external rotation with RMS errors of about 1°. Favre et al. [31] proposed the combination of a functional calibration method and an inertial ambulatory system for knee angle estimation and achieved mean errors of between 1° and 12°. Furthermore, Favre et al. [36] estimated absolute knee flexion/extension, ab-

duction/adduction and relative knee internal/external rotation angles with mean offset errors of -1$\pm$1°, 0$\pm$0.6° and 3.4$\pm$2.7° and mean RMS errors of 1.5$\pm$0.4°, 1.7$\pm$0.5° and 1.6$\pm$0.5°. Takeda et al. [37] used wearable acceleration and gyro sensors to calculate hip flexion/extension and adduction/abduction and knee flexion/extension with RMS errors of $8.7°$, $5.0°$ and $6.8°$ respectively. Finally, Bamberg [38] developed a sophisticated wireless wearable system with an IMU, force sensors and an electric field height sensor and estimated foot pitch mean RMS error of 5.2$\pm$2.0°. Foot progression angle estimation in the present study was more accurate than several gait kinematic estimates in previous work. This is likely due at least in part to static assumption of zero velocity movement of the foot during stance, which is not valid assumption for other body segments during gait.

Kinematic estimation algorithms based solely on accelerometer and gyroscope data are typically prone to drift due to the need to integrate angular velocity data from the gyroscope and double integrate acceleration data from the accelerometer. If the direction and magnitude of drift can be accurately estimated, a predictive model can be used to reduce errors [14]. However, in our case, the direction and magnitude of the resulting drift were difficult to approximate as even small errors in the drift model could create significant foot progression angle errors over time. Thus, instead of a predictive modeling approach, we used magnetometer data not prone to drift to improve overall accuracy and bound estimation errors over time.

In the presented algorithm, the α value acts as a filter for the heading vector giving more or less weight to the current step's heading vector estimation. It suppresses the noise contained in the FPA calculation. There is a tradeoff in selecting the α value. If there was no filter, the FPA estimator would respond very quickly, particularly after turning or changing heading direction, but during straight-line walking it would be less accurate. If the filter value is too high, then the heading vector estimation would be more accurate during straight line walking, but would update very slowly after change in heading directions causing invalid FPA estimates for a significant period. Because FPA is only valid clinically during straight line walking, in our validation experiment, we selected a fixed α value for all subjects based on pilot testing to give a stable FPA estimate for straight line walking. Future work could devise more sophisticated methods for selecting an appropriate α value such as a real-time adapting α value that is subject specific or an α value based on the walking mode (e.g. straight-line walking or turning) which could potentially improve heading vector estimation. Additionally, heading vector estimation could potentially be improved by using absolute positions through GPS for outdoor settings and localized sensor networks of ultra-wideband transmitters/receivers [39], [40] or visual sensing with SLAM [41] for indoor settings.

One limitation of this study is that we only tested healthy subjects with normal gait patterns. The accuracy of the algorithm may decrease for movement disorders with abnormal gaits such as foot drop in individuals with cerebral palsy or foot dragging in some individuals following a stroke. Additionally, because the presented algorithm relies on magnetometer input, it is important to perform proper calibration to get an accurate magnetic north estimate [42]. However, even with proper calibration, the magnetometer could still be susceptible to errors from relatively large unaccounted electromagnetic fields. The foot axis in our algorithm is perpendicular to both the ankle axis of rotation and the vertical axis. In general, this is not the same as a line from the calcareous to the head of the 2nd metatarsal as is assumed to be the foot axis in the motion capture system. When comparing FPA measurements from our algorithm using the magneto-IMU system and the motion capture system, we subtracted this offset. In gait retraining often the most important factor is the change in FPA not the absolute value of FPA, however there may be other applications where the absolute FPA value is critical and in this case further analysis should be performed systematically quantify this offset. In addition, at higher speeds, orientation estimation accuracy of the gradient descent algorithm may deteriorate [24] and the ratio between stance and swing phases will changes, thus caution should be taken when using the algorithm for high-speed walking or running.

In the current implementation, all data processing was done via Matlab on the computer, and we simulated the real-time application scenario by only using data from current and previous time steps. We also performed preliminary testing of this algorithm on a completely portable, wearable system with a STM32F401 MCU (84 MHz) processor, and found that the latency time is 1.7 milliseconds, thus the algorithm could run at a maximum update rate of approximately 588 Hz. A comprehensive study under different conditions such as fast walking, running and ambulating inclined terrain could provide further insights into the algorithm's performance for varying conditions.

VI. Conclusion

In conclusion, we have presented a novel foot progression angle estimation algorithm based on zero-velocity estimation, a complimentary filter and the introduction of real-time heading vector estimation. Validation experimental results demonstrated that the algorithm accurately estimated foot progression angles as compared to standard motion capture estimation for subjects walking in multiple foot orientations and walking speeds. These results could serve as a foundation for future gait research based on wearable systems to assess or train walking patterns outside a laboratory setting in natural walking environments.

Acknowledgments

This work was supported by the National Natural Science Foundation of China (#51505283, #51421092), the Science and Technology Commission of Shanghai Municipality (Yangfan Program, #14YF1401700), the University of MichiganShanghai Jiao Tong University Collaboration on Nanotechnology for Energy and Biomedical Applications (#14X120010006), and the U.S. National Science Foundation through the Human-Centered Computing program (#1017826).

REFERENCES

[1] S. A. Rethlefsen *et al.*, "Causes of intoeing gait in children with cerebral palsy." *The Journal of bone and joint surgery. American volume*, vol. 88, no. 10, pp. 2175–80, Oct. 2006.

[2] P. B. Shull *et al.*, "Six-week gait retraining program reduces knee adduction moment, reduces pain, and improves function for individuals with medial compartment knee osteoarthritis." *Journal of orthopaedic research : official publication of the Orthopaedic Research Society*, vol. 31, no. 7, pp. 1020–5, Jul. 2013.

[3] M. A. Hunt and J. Takacs, "Effects of a 10-week toe-out gait modification intervention in people with medial knee osteoarthritis: a pilot, feasibility study." *Osteoarthritis and cartilage / OARS, Osteoarthritis Research Society*, vol. 22, no. 7, pp. 904–11, Jul. 2014.

[4] V. C. Phan *et al.*, "Foot progression angle after distal tibial physeal fractures." *Journal of pediatric orthopedics*, vol. 22, no. 1, pp. 31–5, Jan. 2002.

[5] D. A. Yngve, "Foot-progression angle in clubfeet." *Journal of pediatric orthopedics*, vol. 10, no. 4, pp. 467–72, Jan. 1990.

[6] M. Andrews *et al.*, "Lower limb alignment and foot angle are related to stance phase knee adduction in normal subjects: a critical analysis of the reliability of gait analysis data." *Journal of orthopaedic research : official publication of the Orthopaedic Research Society*, vol. 14, no. 2, pp. 289–95, Mar. 1996.

[7] M. Guo *et al.*, "The influence of foot progression angle on the knee adduction moment during walking and stair climbing in pain free individuals with knee osteoarthritis." *Gait & posture*, vol. 26, no. 3, pp. 436–41, Sep. 2007.

[8] P. B. Shull *et al.*, "Toe-in gait reduces the first peak knee adduction moment in patients with medial compartment knee osteoarthritis." *Journal of biomechanics*, vol. 46, no. 1, pp. 122–8, Jan. 2013.

[9] K. A. Bowsher and C. L. Vaughan, "Effect of foot-progression angle on hip joint moments during gait," *Journal of Biomechanics*, vol. 28, no. 6, pp. 759–762, Jun. 1995.

[10] Y.-C. Lai *et al.*, "Impact of foot progression angle on the distribution of plantar pressure in normal children." *Clinical biomechanics (Bristol, Avon)*, vol. 29, no. 2, pp. 196–200, Feb. 2014.

[11] M. K. Hastings *et al.*, "Foot progression angle and medial loading in individuals with diabetes mellitus, peripheral neuropathy, and a foot ulcer." *Gait & posture*, vol. 32, no. 2, pp. 237–41, Jun. 2010.

[12] I. P. I. Pappas *et al.*, "A reliable gait phase detection system," *IEEE Transactions on Neural Systems and Rehabilitation Engineering*, vol. 9, no. 100, pp. 113–125, 2001.

[13] A. M. Sabatini *et al.*, "Assessment of walking features from foot inertial sensing." *IEEE transactions on bio-medical engineering*, vol. 52, no. 3, pp. 486–94, Mar. 2005.

[14] J. R. Rebula *et al.*, "Measurement of foot placement and its variability with inertial sensors." *Gait & posture*, Jun. 2013.

[15] H. Rouhani *et al.*, "Measurement of Multi-segment Foot Joint Angles During Gait Using a Wearable System," *Journal of Biomechanical Engineering*, vol. 134, no. June 2012, p. 061006, 2012.

[16] B. Mariani *et al.*, "On-shoe wearable sensors for gait and turning assessment of patients with parkinson's disease," *IEEE Transactions on Biomedical Engineering*, vol. 60, no. 1, pp. 155–158, 2013.

[17] I. Tien *et al.*, "Results of using a wireless inertial measuring system to quantify gait motions in control subjects," *IEEE Transactions on Information Technology in Biomedicine*, vol. 14, no. 4, pp. 904–915, 2010.

[18] H. M. Schepers *et al.*, "Ambulatory assessment of ankle and foot dynamics," *IEEE Transactions on Biomedical Engineering*, vol. 54, no. 5, pp. 895–902, 2007.

[19] H. Rouhani *et al.*, "A wearable system for multi-segment foot kinetics measurement." *Journal of biomechanics*, vol. 47, no. 7, pp. 1704–11, May 2014.

[20] X. Meng *et al.*, "Self-contained pedestrian tracking during normal walking using an inertial/magnetic sensor module." *IEEE transactions on bio-medical engineering*, vol. 61, no. 3, pp. 892–9, Mar. 2014.

[21] X. Yun *et al.*, "Estimation of Human Foot Motion During Normal Walking Using Inertial and Magnetic Sensor Measurements," *IEEE Transactions on Instrumentation and Measurement*, vol. 61, no. 7, pp. 2059–2072, Jul. 2012.

[22] S. Kwanmuang *et al.*, "Magnetometer-enhanced personal locator for tunnels and GPS-denied outdoor environments," *Proceedings of SPIE - The International Society for Optical Engineering*, vol. 8019, pp. The Society of Photo–Optical Instrumentation Engin, 2011.

[23] A. M. Sabatini, "Quaternion-based extended Kalman filter for determining orientation by inertial and magnetic sensing." *IEEE transactions on bio-medical engineering*, vol. 53, no. 7, pp. 1346–56, Jul. 2006.

[24] S. O. H. Madgwick *et al.*, "Estimation of IMU and MARG orientation using a gradient descent algorithm," *IEEE International Conference on Rehabilitation Robotics*, pp. 179–185, 2011.

[25] I. Skog *et al.*, "Zero-velocity detection — an algorithm evaluation." *IEEE transactions on bio-medical engineering*, vol. 57, no. 11, pp. 2657–2666, Jul. 2010.

[26] B. Mariani *et al.*, "Quantitative estimation of foot-flat and stance phase of gait using foot-worn inertial sensors." *Gait & posture*, vol. 37, no. 2, pp. 229–34, Feb. 2013.

[27] P. B. Shull *et al.*, "Quantified self and human movement: A review on the clinical impact of wearable sensing and feedback for gait analysis and intervention," *Gait & Posture*, vol. 40, no. 1, pp. 11–19, Apr. 2014.

[28] D. J. Rutherford *et al.*, "Foot progression angle and the knee adduction moment: a cross-sectional investigation in knee osteoarthritis." *Osteoarthritis and cartilage / OARS, Osteoarthritis Research Society*, vol. 16, no. 8, pp. 883–9, Aug. 2008.

[29] J. Bortz, "A New Mathematical Formulation for Strapdown Inertial Navigation," *IEEE Transactions on Aerospace and Electronic Systems*, vol. AES-7, no. 1, pp. 61–66, Jan. 1971.

[30] K. W. Spring, "Euler parameters and the use of quaternion algebra in the manipulation of finite rotations: A review," *Mechanism and Machine Theory*, vol. 21, no. 5, pp. 365–373, Jan. 1986.

[31] J. Favre *et al.*, "3D joint rotation measurement using MEMs inertial sensors : Application to the knee joint," *Measurement*, pp. 3–6, 2006.

[32] M. Simic *et al.*, "Altering foot progression angle in people with medial knee osteoarthritis: The effects of varying toe-in and toe-out angles aremediated by pain and malalignment," *Osteoarthritis and Cartilage*, vol. 21, no. 9, pp. 1272–1280, Sep. 2013.

[33] C. K. Cochrane *et al.*, "Biomechanical mechanisms of toe-out gait performance in people with and without knee osteoarthritis," *Clinical Biomechanics*, vol. 29, no. 1, pp. 83–86, 2014.

[34] M. Hunt and J. Takacs, "Effects of a 10-week toe-out gait modification intervention in people with medial knee osteoarthritis: a pilot, feasibility study," *Osteoarthritis and Cartilage*, vol. 22, no. 7, pp. 904–911, 2014.

[35] D. Roetenberg *et al.*, "Ambulatory position and orientation tracking fusing magnetic and inertial sensing," *IEEE Transactions on Biomedical Engineering*, vol. 54, no. 5, pp. 883–890, 2007.

[36] J. Favre *et al.*, "Ambulatory measurement of 3D knee joint angle," *Journal of Biomechanics*, vol. 41, pp. 1029–1035, 2008.

[37] R. Takeda *et al.*, "Gait posture estimation by wearable acceleration and gyro sensor," *IFMBE Proceedings*, vol. 25, no. 15, pp. 111–114, 2009.

[38] S. J. M. Bamberg *et al.*, "Gait analysis using a shoe-integrated wireless sensor system." *IEEE transactions on information technology in biomedicine : a publication of the IEEE Engineering in Medicine and Biology Society*, vol. 12, no. 4, pp. 413–423, 2008.

[39] J. D. Hol *et al.*, "Tightly coupled UWB/IMU pose estimation," in *2009 IEEE International Conference on Ultra-Wideband*, vol. 2009. IEEE, Sep. 2009, pp. 688–692.

[40] J. a. Corrales *et al.*, "Hybrid tracking of human operators using IMU/UWB data fusion by a Kalman filter," in *Proceedings of the 3rd international conference on Human robot interaction - HRI '08*. New York, New York, USA: ACM Press, 2008, p. 193.

[41] G. Nützi *et al.*, "Fusion of IMU and Vision for Absolute Scale Estimation in Monocular SLAM," *Journal of Intelligent & Robotic Systems*, vol. 61, no. 1-4, pp. 287–299, Nov. 2010.

[42] J. F. Vasconcelos *et al.*, "Geometric Approach to Strapdown Magnetometer Calibration in Sensor Frame," *IEEE Transactions on Aerospace and Electronic Systems*, vol. 47, no. 2, pp. 1293–1306, Apr. 2011.

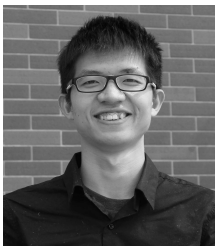

Yangjian Huang received the B.S. in Mechanical Engineering from Donghua University in 2013. He is currenly a PhD student in the State Key Laboratory of Mechanical System and Vibration, School of Mechanical Engineering at Shanghai Jiao Tong University. His interests include wearable systems, motion tracking and retraining, and inertial position navigation.

Wisit Jirattigalachote received the B.S. in Mechanical Engineering from University of Michigan in 2008 and the Ph.D. degree in Mechanical Engineering from Stanford University in 2015. His interests include wearable electronics, human motion sensing and training, and rehabilitation robotics.

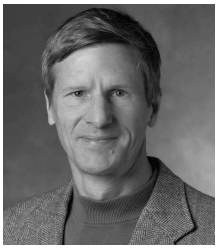

Mark R. Cutkosky received the B.S. in Mechanical Engineering from University of Rochester in 1978 and the Ph.D. degree in Mechanical Engineering from Carnegie-Mellon University in 1985. His interests include robotic hands manipulation, tactile sensors of human/computer interaction, rapid prototyping.

Xiangyang Zhu Xiangyang Zhu received the B.S. degree from the Department of Automatic Control Engineering, Nanjing Institute of Technology, Nanjing, China, in 1985, the M.Phil. degree in instrumentation engineering and the Ph.D. degree in automatic control engineering, both from Southeast University, Nanjing, China, in 1989 and 1992, respectively. From 1993 to 1994, he was a Postdoctoral Research Fellow with the Huazhong University of Science and Technology, Wuhan, China. In 1995, he joined the Department of Mechanical Engineering, Southeast University, as an Associate Professor. Since June 2002, he has been with the School of Mechanical Engineering, Shanghai Jiao Tong University, Shanghai, China, where he is currently a Changjiang Chair Professor and the Director of the Robotics Institute. His current research interests include robotic manipulation planning, humanmachine interfacing, and biomechatronics.

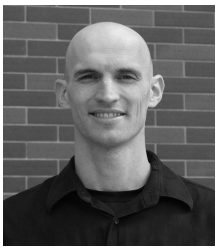

Peter B. Shull received the B.S. in Mechanical Engineering and Computer Engineering from LeTourneau University in 2005 and the Ph.D. degree in Mechanical Engineering from Stanford University in 2012. His interests include wearable systems, real-time movement sensing and feedback, gait retraining, and biomechanics.